JACS
JOURNAL OF THE AMERICAN CHEMICAL SOCIETY
Article
pubs.acs.org/JACS

Biomimetic Oxygen Reduction by Cofacial Porphyrins at a Liquid–Liquid Interface

Pekka Peljo,[†] Lasse Murtomäki,*[,†] Tanja Kallio,[†] Hai-Jun Xu,[‡] Michel Meyer,[‡] Claude P. Gros,[‡] Jean-Michel Barbe,[‡] Hubert H. Girault,[§] Kari Laasonen,[†] and Kyösti Kontturi[†]

[†]Department of Chemistry, Aalto University, P.O. Box 16100, 00076 Aalto, Finland

[‡]Institut de Chimie Moléculaire de l'Université de Bourgogne (ICMUB), UMR CNRS 6302, 9 avenue A. Savary, BP 47870, 21078 Dijon Cedex, France

[§]Laboratoire d'Electrochimie Physique et Analytique, Ecole Polytechnique Fédérale de Lausanne (EPFL), Station 6, CH-1015 Lausanne, Switzerland

Supporting Information

ABSTRACT: Oxygen reduction catalyzed by cofacial metalloporphyrins at the 1,2-dichlorobenzene–water interface was studied with two lipophilic electron donors of similar driving force, 1,1′-dimethylferrocene (DMFc) and tetrathiafulvalene (TTF). The reaction produces mainly water and some hydrogen peroxide, but the mediator has a significant effect on the selectivity, as DMFc and the porphyrins themselves catalyze the decomposition and the further reduction of hydrogen peroxide. Density functional theory calculations indicate that the biscobaltporphyrin, 4,5-bis[5-(2,8,13,17-tetraethyl-3,7,12,18-tetramethylporphyrinyl)]-9,9-dimethylxanthene, Co_2(DPX), actually catalyzes oxygen reduction to hydrogen peroxide when oxygen is bound on the "exo" side ("dock-on") of the catalyst, while four-electron reduction takes place with oxygen bound on the "endo" side ("dock-in") of the molecule. These results can be explained by a "dock-on/dock-in" mechanism. The next step for improving bioinspired oxygen reduction catalysts would be blocking the "dock-on" path to achieve selective four-electron reduction of molecular oxygen.

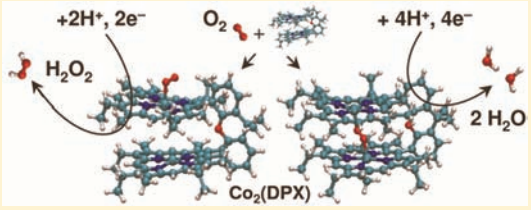

INTRODUCTION

In nature, several important reactions take place at membrane boundaries. For example, the oxygen reduction reaction (ORR) in the cell respiration chain is catalyzed by enzymes bound in the hydrophobic lipid bilayer of the mitochondrial membranes. These enzymes contain porphyrin subunits as active centers. Since the first report regarding the catalytic activity of cobalt phthalocyanine toward oxygen reduction,[1] different porphyrins and other N_4-macrocyclic metal complexes have been studied extensively as possible catalysts of oxygen reduction.[2,3] A common way to study the ORR has been to attach the catalyst to a carbon electrode.[3,4] Alternatively, homogeneous oxygen reduction may be studied in nonaqueous media because the catalysts are insoluble in water. However, this approach requires the use of organic acids. Simple metalloporphyrins were shown to catalyze oxygen reduction to hydrogen peroxide by ferrocene in acetonitrile,[5,6] while cofacial biscobalt bisporphyrins catalyzed this reduction to water in benzonitrile.[7] Similar results were obtained in heterogeneous electrocatalysis with cofacial porphyrins.[8] Cofacial porphyrins are also interesting because of their structural similarity with cytochrome *c* oxidase (C*c*O), the enzyme responsible for the selective four-electron reduction of molecular oxygen in nature. The active center of C*c*O consists of an iron porphyrin/copper heterodinuclear center, where a copper atom coordinated by three histidines is located above the iron center of the heme.[9]

The question remains whether the above-mentioned experiments can be translated into a deeper understanding of biology. The respiratory chain is quite complex, as it includes transfer of protons and electrons across the interface between the hydrophobic lipid bilayer and an aqueous phase.[2] An interface between two immiscible electrolyte solutions (ITIES) provides a biomimetic approach to study these systems.[10] Electrochemistry at the ITIES enables the monitoring of ion and electron transfers, which are elementary processes in cellular traffic,[11] and has, therefore, been used to study ORR by molecular electron donors at a liquid–liquid interface.[12−24] A key finding was that the interfacial Galvani potential difference could be used to drive protons from the aqueous to the oil phase, thus enabling the reduction of oxygen to hydrogen peroxide by decamethylferrocene (DcMFc).[16] To increase reaction rates, organic bases like dodecylaniline have been used to facilitate proton transfer to the organic phase and thus catalyze oxygen reduction by decamethylferrocene.[17] Voltammetry at liquid–liquid interfaces is an efficient tool to study different porphyrins as ORR molecular electrocatalysts.[18−21,25] This catalyzed reaction includes a biphasic proton-coupled electron transfer (PCET) involving aqueous protons and electron donors (for example decamethylferrocene) in the oil

Received: January 16, 2012
Published: March 15, 2012

dx.doi.org/10.1021/ja3004914 | J. Am. Chem. Soc. 2012, 134, 5974−5984

phase. The rate of the reaction is controlled by the Galvani potential difference across the interface. The role of the molecular catalyst is to bind molecular oxygen at the interface, the complex having a high affinity for aqueous protons and electrons.

In this Article, different cofacial porphyrins are considered as molecular catalysts for oxygen reduction at liquid−liquid interfaces. The selectivity of these catalysts toward the four-electron reduction of oxygen by two lipophilic electron donors of similar driving force, 1,1′-dimethylferrocene (DMFc)[18,19] and tetrathiafulvalene (TTF),[26] was investigated. Both are known to react very slowly with oxygen, but ferrocene derivatives are known to react with hydrogen peroxide,[27] while TTF has been shown to be inactive.[26] The effect of the mediator on hydrogen peroxide decomposition may be distinguished using the two aforementioned reducing agents. We found that all of the studied catalysts promote oxygen reduction both to hydrogen peroxide and to water at the liquid−liquid interface. However, the electron donor has a significant effect on the observed selectivity as DMFc also catalyzes the decomposition of hydrogen peroxide. To explain these results, ORR catalyzed by Co_2(DPX) was investigated in more detail by density functional theory (DFT) calculations, and a "dock-on/dock-in" mechanism accounting for the different pathways is proposed.

EXPERIMENTAL SECTION

Chemicals. All chemicals were used as received. The aqueous solutions were prepared with ultrapure water (Millipore Milli-Q, specific resistivity 18.2 MΩ cm). Solvents were 1,2-dichlorobenzene (DCB, ≥98%, Fluka), 1,2-dichloroethane (DCE, 99.9%, Merck), HCl (FF Chemicals, 1 M), ethanol (94%, Altia), and acetone (99.5%, Lab Scan). 1,1′-Dimethylferrocene (DMFc, 97%, Aldrich) and tetrathiafulvalene (TTF, 99+%, Acros) were used as redox mediators. Other chemicals include sodium iodide (99%, Acros), potassium bis(oxalato)oxotitanate(IV) dihydrate (TiOx, Alfa Aesar), and tetraethylammonium chloride (TEACl, 98%, Sigma).

5,10,15,20-*meso*-Tetraphenylporphyrin cobalt (CoTPP), biscobaltporphyrins of 4,5-bis[5-(2,8,13,17-tetraethyl-3,7,12,18-tetramethylporphyrinyl)]-9,9-dimethylxanthene (Co_2(DPX)), 2,2′-bis[5-(2,8,13,17-tetraethyl-3,7,12,18-tetramethylporphyrinyl)] diphenylether (Co_2(DPOx)), and 4,6-bis[5-(2,8,13,17-tetraethyl-3,7,12,18-tetramethylporphyrinyl)] dibenzofuran (Co_2(DPO)) were synthesized as described earlier.[25,28]

Lithium tetrakis(pentafluorophenyl)borate (LiTB) *n*-etherate (Boulder Scientific Company) and bis(triphenylphosphoranylidene) ammonium chloride (BACl, 97%, Aldrich) were used to prepare bis(triphenylphosphoranylidene) ammonium tetrakis(pentafluorophenyl)borate (BATB) by metathesis of aqueous equimolar solutions of BACl and LiTB. The resulting precipitates were filtered, washed, and recrystallized from acetone:ethanol (1:1) mixture.[29]

Electrochemical Measurements. All of the electrochemical measurements were performed at ambient temperature (20 ± 2 °C) under aerobic conditions in a Faraday cage. Cyclic voltammograms (CVs) at the water−DCB interface were recorded with an Autolab four-electrode potentiostat PGSTAT100 (EcoChemie, The Netherlands) at the scan rate of 50 mV/s. A glass cell designed for liquid−liquid interface experiments with an interfacial area of 0.159 cm^2 was a generous gift from professor Zdeněk Samec, J. Heyrovský Institute of Physical Chemistry, Prague. The cell is shown in Figure 1. Two reference electrodes (RE, Ag/AgCl), placed in Luggin capillaries to reduce *iR* drop, controlled the potential difference across the interface, while the tungsten counter electrodes (CE) in both phases provided electric current. The organic reference phase had a common cation with the supporting electrolyte of the organic phase. The potential was converted to the Galvani potential difference ($\Delta_o^w\phi$) based on cyclic voltammetry measurement of the reversible half-wave potential of the TEA^+ (0.116 V in DCB)[30] or $DMFc^+$ (−0.024 V in DCB)[31] ion transfer.

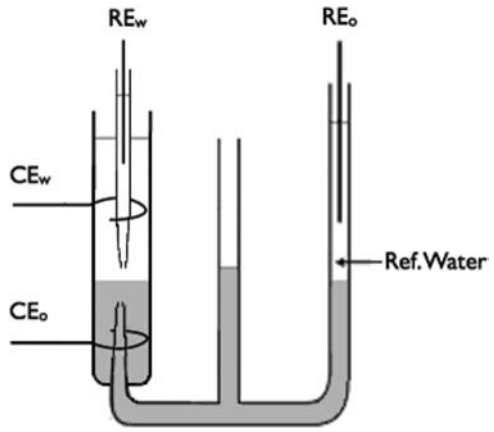

Figure 1. The four-electrode cell used for the CV measurements. The oil phase is shown shaded.

DMFc was used as a mediator, because it does not have significant activity toward oxygen reduction. Four-electrode cell measurements were used to compare the catalytic activity of CoTPP and cofacial "Pacman" porphyrins (Co_2(DPX), Co_2(DPO), and Co_2(DPOx)) toward oxygen reduction. A CoTPP concentration of 1 mM was needed to observe any catalytic activity, but a concentration of 100 μM was enough for cofacial porphyrins. The HCl concentration of the aqueous phase was varied between 0.01 and 1 M, as described in Scheme 1.

Scheme 1. Electrochemical Cell Used for the CV Measurements[a]

Ag	AgCl	10 mM LiCl 1 mM BACl	5 mM BATB 5 mM DMFc y μM catalyst	0.01-1 M HCl	AgCl	Ag
		Ref. Water	Oil	Water		

[a] *y* was 100 for cofacial porphyrins and 1000 for CoTPP.

To elucidate the mechanism of oxygen reduction by these catalysts, the effects of nitrogen, oxygen, protons, and DMFc on the absorption spectra of 10 μM CoTPP and Co_2(DPOx) solutions were investigated by UV−vis spectrophotometry, using a Varian Cary 50 Conc spectrophotometer and a quartz cuvette with an optical path length of 1 cm. Catalyst solutions were saturated with nitrogen, and then with oxygen, followed by dropwise addition of HTB solution, prepared as described elsewhere,[32] and 2 mM DMFc solution.

Two-Phase Reactions with Chemically Controlled Polarization. The interface was polarized with the distribution of a common ion (TB^-) across the interface in so-called shake-flask experiments. 2.0 mL of DCB or DCE solution containing the lipophilic electron donor (TTF or DMFc), catalyst, and supporting electrolyte, and an equal amount of acidic aqueous solution containing LiTB, were added into a vial. The composition of the cell is illustrated in Scheme 2.

The mixture was stirred with a magnetic stirrer for different reaction times and left to settle for 30 s. After phase separation, the aqueous phase was analyzed for hydrogen peroxide with the NaI method: solid NaI was added to 1 mL of the aqueous phase (NaI concentration of 0.1 M) and left to react for 30 min in the dark, by which time the hydrogen peroxide present oxidized iodide to I_3^-.[16] The absorbance of triiodide was measured at 352 nm using a Varian Cary 50 Conc spectrophotometer and a quartz cuvette with an optical path length of 0.1 cm. The same setup was used for all UV−vis measurements.

dx.doi.org/10.1021/ja3004914 | J. Am. Chem. Soc. 2012, 134, 5974−5984

Scheme 2. Schematic Representation of the Initial Composition of the Aqueous Phase and the Organic Phase for the Biphasic Oxygen Reduction Experiments

5 mM BATB	‖	5 mM LiTB
2 mM DMFc	‖	10 mM HCl
100 μM catalyst	‖	
Oil	‖	Water

Alternatively, the H_2O_2 content was analyzed with titanium oxalate: a 1 mL sample was acidified with sulfuric acid and mixed with a potassium titanium oxalate solution, which reacts with hydrogen peroxide to form a yellow complex. The absorbance was measured at 400 nm[33] (optical path length of 1 cm). Spectra of the organic phase were recorded before and after reaction. Oxygen solubility in DCB is not known, but its concentration in chlorobenzene saturated with air at room temperature is 1.62 mM[34] and the value in DCE is 1.38 mM.[35] A mediator concentration of 2 mM was used because it is the limiting factor for oxygen reduction, as more than 2.8 mM of electron donor would be needed for complete two-electron reduction.

Scheme 3. Schematic Representation of the Initial Composition of the Aqueous Phase and the Organic Phase for the Biphasic Hydrogen Peroxide Decomposition (A) and Reduction (B) Experiments

A			B		
5 mM BATB	‖	1 mM H_2O_2	5 mM BATB	‖	1 mM H_2O
2 mM DMFc	‖	10 mM HCl	2 mM DMFc	‖	5 mM LiTB
100μM Co_2(DPX)	‖		100 μM Co_2(DPX)	‖	10 mM HCl
or 1 mM CoTPP	‖				
Oil	‖	Water	Oil	‖	Water

The stability of hydrogen peroxide in the aqueous phase was studied with biphasic experiments, with the cell shown in Scheme 3A. The mixture was stirred and the hydrogen peroxide concentration determined after 1 and 10 min of reaction with the titanium oxalate method described above. The reduction of hydrogen peroxide was investigated in a glovebox under nitrogen atmosphere, with the cell composition shown in Scheme 3B. The mixture of 2 mL of both phases was stirred for 60 s. After 30 s of settling time, the aqueous phase was separated and assayed for hydrogen peroxide with the titanium oxalate method.

Ultramicroelectrode Measurements. To determine the amount of redox mediator consumed during the reaction, the ratio of oxidized and neutral species was deduced from cyclic voltammetry measurements performed on a CHI900 electrochemical workstation (CH Instruments, Austin, TX), at a scan rate of 20 mV s^{-1} using 25 μm Pt or 10 μm carbon fiber ultramicroelectrodes (UME) and a platinum wire counter electrode. The same setup was used to determine the formal redox potentials of TTF in DCB, using decamethylferrocene as a reference. Fabrication of the Pt and carbon fiber UMEs was performed as previously described.[36] Briefly, a Pt wire or a carbon fiber (Goodfellow, Oxford, UK) was sealed inside the tip of a glass capillary (i.e., inner diameter 1 mm, outer diameter 1.5 mm, Biologic) with a Bunsen burner. The sealed capillary was subjected to a vacuum for more than 30 min, and the glass sealing of the Pt wire or carbon fiber was improved by slow heating with a resistor heater coil (model 720, David Kopf Instruments, U.S.). The electrical connection to a tin/copper wire was made with tin powder.

Computational Details. The GPAW[37] code was used to study oxygen adsorbed on cofacial biscobalt bisporphyrin Co_2(DPX). The Density Functional Theory (DFT) with the Generalized Gradient corrections (GGA) approach was used, as well as the Perdew, Burke, and Ernzerhof (PBE) model[38] for the exchange and correlation. The DFT-GGA is a reliable approximation for organometallic systems.[39] The wave functions were expressed using numerical grid type basis function and PAW pseudopotentials,[40] and spin unrestricted scheme was used in all of the cases. The used grid spacing was 0.2 bohr. Also, the total value of spin was not constrained. In all of the cases, the geometry of the molecules was optimized. The molecules were placed in periodic boxes of 20 Å. The effect of periodicity is very small because some calculations were done without the periodicity.

RESULTS AND DISCUSSION

Four-Electrode Cell Measurements. Figure 2 shows the *iR* compensated voltammograms of 1 mM CoTPP with 5 mM DMFc at various pH values. For CoTPP, a reversible transfer of $DMFc^+$ (peak separation of ca. 60 mV) is observed at ca. 0 V (IT region in Figure 2) showing that DMFc is oxidized by oxygen in the presence of CoTPP. Reversible chloride transfer takes place at the negative end of the window, and an irreversible current wave can be attributed to a PCET reaction at the positive limit of the window; that is, protons are consumed according to eq 1 and/or 2[18] (PCET region in Figure 2, D stands for a lipophilic electron donor, o for the oil phase, and w for the aqueous phase). The voltammograms without any catalyst resemble the baseline (data not shown) meaning that DMFc is not oxidized on its own on the time scale of the experiment.[31]

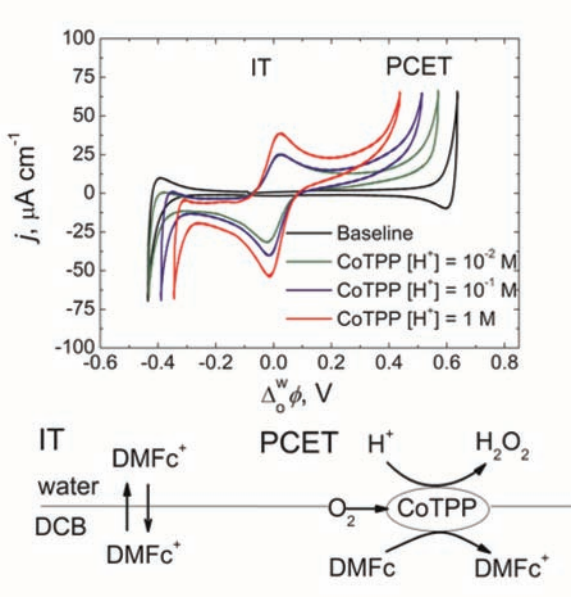

Figure 2. Cyclic voltammograms of 1 mM CoTPP with 5 mM DMFc and 5 mM BATB in DCB for various proton concentrations in the aqueous phase. The baseline corresponds to the CV of 5 mM BATB in DCB in contact with 10 mM aqueous HCl. Below: Mechanisms of ion transfer (IT) and proton coupled electron transfer (PCET).[41]

$$2D(o) + O_2(o) + 2H^+(o) \xrightarrow{cat.} 2D^+(o) + H_2O_2(w) \quad (1)$$

$$4D(o) + O_2(o) + 4H^+(o) \xrightarrow{cat.} 4D^+(o) + 2H_2O(w) \quad (2)$$

The complex CoTPP–O_2 has a low affinity for protons, as indicated by the PCET wave at 0.55 V at pH 2. A dependence of the transfer potentials of chloride and PCET of ca. 60 mV

dx.doi.org/10.1021/ja3004914 | J. Am. Chem. Soc. 2012, 134, 5974–5984

versus log [HCl] is observed, proving that measurements were properly *iR* compensated.

Figure 3 shows the voltammograms of 100 μM Co_2(DPOx), Co_2(DPO), and Co_2(DPX). All tested cofacial bisporphyrins

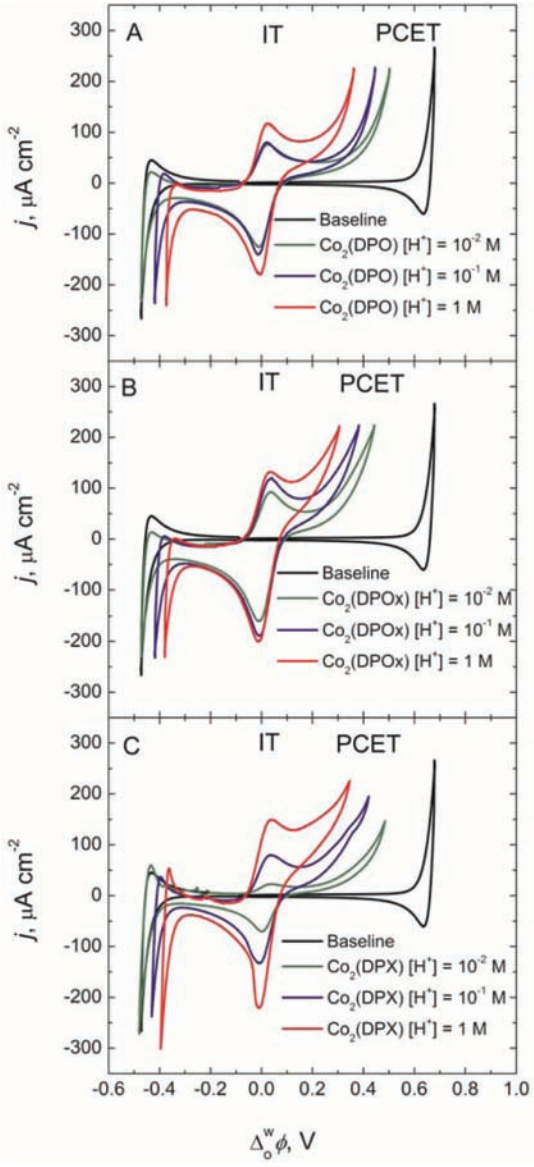

Figure 3. Cyclic voltammograms of 100 μM Co_2(DPO) (A), Co_2(DPOx) (B), and Co_2(DPX) (C) with 5 mM DMFc and 5 mM BATB in DCB for various proton concentrations in the aqueous phase. The baseline corresponds to the CV of 5 mM BATB in DCB in contact with 10 mM aqueous HCl.

exhibit a high catalytic activity toward oxygen reduction as indicated by the large amount of $DMFc^+$ formed. The amount of catalyst required is far less than that of CoTPP, while obtained current densities are considerably higher. No catalytic activity was observed in the absence of a redox mediator (Supporting Information, Figure S-1). On the basis of these voltammetric measurements, Co_2(DPOx) appears to be the best ORR catalyst among the three tested cofacial bisporphyrins at the liquid–liquid interface.

The catalyst plays two roles in the present system: it coordinates an oxygen molecule at the metal center so that both electron and proton transfer reactions can take place; that is, it activates the O–O bond by lowering the energy barrier for electron transfer and reacts with the protons and the electron donors.

The results of Figure 3 show that Co_2(DPOx)–O_2 reacts by PCET at 0.4 V at pH 2. The other complexes Co_2(DPO)–O_2 and Co_2(DPX)–O_2 behave quite similarly but with PCET wave at 0.5 V at pH 2. In all cases, the onset potential varies by 60 mV/pH, indicating a PCET reaction characterized by the absence of a return peak upon scan reversal. In the absence of a mediator, the voltammogram does not differ significantly from the baseline (Supporting Information, Figure S-1). A wave corresponding to the facilitated transport of chloride is observed for Co_2(DPOx) and Co_2(DPX) at 0 V. This wave shifts to more positive potentials with the increase of the chloride concentration (60 mV/decade), confirming that the wave indeed originates from the facilitated chloride transfer (proton transfer wave would shift to the opposite direction).

Oxygen reduction at a single porphyrin unit can be rationalized by the scheme proposed by Partovi-Nia et al. (Supporting Information, Scheme S-1),[19] where the oxygen–metalloporphyrin complex takes protons from the aqueous phase and electrons from the donor in the oil phase in a PCET step. The formed hydrogen peroxide is extracted into the aqueous phase. The reduction of O_2 catalyzed by cofacial porphyrins is described by the scheme proposed by Nocera et al. (Supporting Information, Scheme S-2).[8] This mechanism is also similar to the one suggested by Fukuzumi et al.[7] Here, reduction of the superoxo complex, $[Co_2O_2]^+$, leads to hydrogen peroxide production, while protonation of the core bypasses the peroxide route resulting in water formation.

To understand the mechanism of oxygen reduction by these catalysts, additional UV–vis measurements were performed using 10 μM solutions of CoTPP and Co_2(DPOx). CoTPP shows an intense Soret band at 416 nm and a quite weak Q-band at 530 nm, while Co_2(DPOx) is characterized by peaks at 330, 395 nm (Soret bands, strong), 527 and 559 nm (Q-bands). Oxygen binding to these porphyrins is strong enough that it cannot be released by bubbling nitrogen through the solution; the presence of oxygen was confirmed by UME measurements. Dropwise addition of a strong organic acid HTB prepared according to the procedure described in ref 31 to the solution resulted in a red shift of the absorption bands (Figures 4 and 5). This indicated that a proton binds to the oxygenated macrocyclic complex as described in Schemes S-1 and S-2. Saturation of the solution by nitrogen or oxygen has no effect on the spectra.

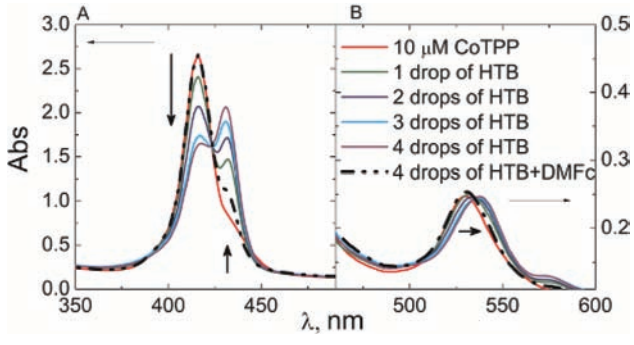

Figure 4. The effect of proton and DMFc additions on the Soret (A) and Q-bands (B) of 10 μM CoTPP in DCB. l = 1 cm. The absorbance scale (0.1–0.5) for Q-band is shown on the right.

dx.doi.org/10.1021/ja3004914 | J. Am. Chem. Soc. 2012, 134, 5974–5984

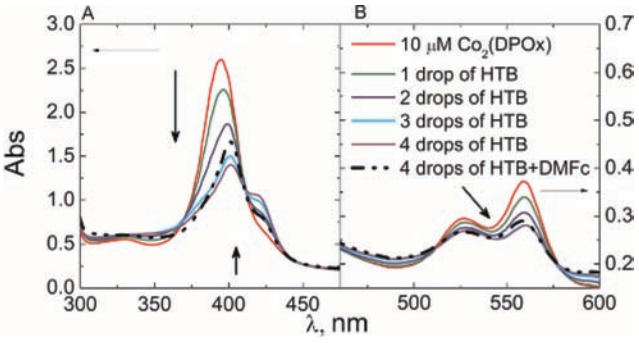

Figure 5. The effect of proton and DMFc additions on the Soret (A) and Q-bands (B) of 10 μM Co_2(DPOx) in DCB. l = 1 cm. The absorbance scale (0−0.7) for Q-bands is shown on the right.

Addition of a small amount of DMFc restored the spectrum of CoTPP, indicating that oxygen reduction took place, consuming protons in the solution and restoring the catalyst to the original state. The absorption spectrum of Co_2(DPOx) was not restored with the addition of DMFc, indicating that cofacial porphyrins undergo irreversible changes during the catalytic cycle, probably due to oxidation of one of the metal centers, as described in Scheme S-2. If more HTB was added (20 drops), the intensity of both Soret and Q-bands continued to decrease and move to lower energies, giving rise to a new band at 625 nm. These results are in agreement with the proposed reaction schemes, indicating that cobalt porphyrin binds the oxygen molecule. The resulting complex is eager to accept protons before undergoing oxidation. These combined reactions are here called PCET as voltammetry cannot differentiate these elementary steps.

Two-Phase Reactions with Chemically Controlled Polarization. The selectivity of different catalysts toward four-electron reduction of molecular oxygen was studied in biphasic reactions, where the Galvani potential difference was determined by the partitioning of a common ion, TB^- (Scheme 2). The Galvani potential difference across the interface was calculated to be 0.658 V[31] (see Supporting Information). Addition of LiTB in the aqueous phase drives protons to the interface and into the oil phase where they can react with the electron donor in the presence of the catalyst. When the protons react, $DMFc^+$ or TTF^+ ions are produced until the electron donor (D) is completely depleted. Partitioning of D^+ between both phases affects the Galvani potential difference. If DMFc is used, the potential is calculated to be 0.641 V at the end of the reaction, sufficient to retain $DMFc^+$ in the oil phase. The composition of both phases at equilibrium at the beginning and at the end of the reaction is reported in the Supporting Information.

Redox potentials of both $TTF/TTF^{\cdot+}$ and $TTF^{\cdot+}/TTF^{2+}$ couples were determined as 0.58 and 1.60 V vs SHE in DCB, respectively (0.56 V vs SHE in DCE),[26] and the value for DMFc is 0.57 V vs SHE,[31] so that the thermodynamic driving force for oxygen reduction is almost the same with these two mediators. For all catalysts considered herein, the observed color change was immediate when the aqueous and oil phases were combined. Figure 6 shows the UV−vis spectra of the oil phase before and after the reaction, for a contact time of 30 s. The inset shows the UME voltammograms (vs $DMFc/DMFc^+$) recorded before and after the reaction to determine the amount of mediator consumed during the reaction catalyzed by Co_2(DPX).

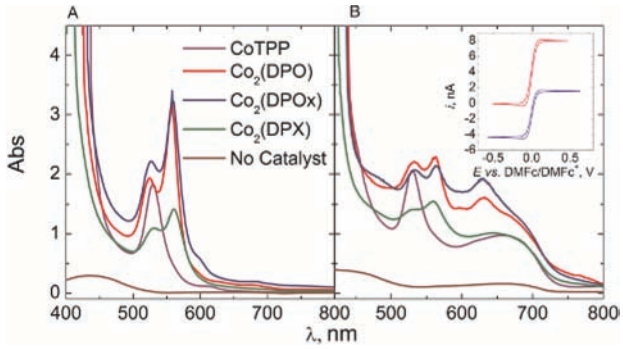

Figure 6. UV−vis spectra of DCB phases containing 100 μM of catalyst, 2 mM DMFc, and 5 mM BATB before (A) and after (B) two-phase reactions. The inset shows the measured UME voltammograms (vs $DMFc/DMFc^+$) before and after two-phase reaction, using 100 μM Co_2(DPX) as a catalyst. The reaction time was 30 s, followed by a 30 s settling time.

The spectral changes occurring in the Soret and Q-band regions of the catalyst are similar to the ones observed on addition of HTB to a solution of the pure porphyrins (Figures 4 and 5), indicating the protonation of the oxygenated complexes in the oil phase. Because DMFc has an absorbance peak at 439 nm and $DMFc^+$ has a broad peak at 550−725 nm (see Supporting Information), the spectral features appearing above 600 nm in Figure 6B unambiguously show that DMFc is oxidized during the experiment. Curiously, the peak at 625 nm is not observed for Co_2(DPO). The reaction ended after all DMFc was oxidized, as the concentration of the electron donor was the limiting factor. The amount of produced hydrogen peroxide was determined along with the amount of consumed electron donor to estimate the stoichiometry of the oxygen reduction reaction, as described above. Electron donor consumption was measured by microelectrode voltammetry (D = 7.09 × 10^{-6} cm^2 s^{-1} for DMFc and 5.89 × 10^{-6} cm^2 s^{-1} for TTF).[31] The percentages of electron donor consumed during the shake flask experiment, as well as the percentages of electron donor used for hydrogen peroxide production and the total number of transferred electron per reduced molecular oxygen, are given in Table 1 for both H_2O_2 analytical methods.

All of the catalysts under consideration showed reasonable selectivity toward four-electron reduction of molecular oxygen after 1 min of reaction, the best one being Co_2(DPX) (NaI method). Overall, the results of Table 1 obtained by two different analytical methods are in reasonable agreement, considering the low amounts of titrated hydrogen peroxide. The slight deviations might arise from the fact that the NaI method is more sensitive (ε = 27 600 M^{-1} cm^{-1})[16] than the TiOx assay (ε = 935 M^{-1} cm^{-1})[33] and is therefore more reliable for determining low H_2O_2 concentrations. Moreover, the relative experimental error associated with the latter method is quite larger with respect to the former one, primarily because of the lower absorbance readings and, as a matter of fact, by the larger impact of the perturbations induced by the presence of small droplets of immiscible organic solvent in the aqueous test solution. On the other hand, the NaI test can be interfered by other oxidizing species, so the TiOx method should be more specific. The uncertainty for the percentage of hydrogen peroxide production resulting from the inaccurate absorbance readings for the NaI method was estimated as 1%, while the value for TiOx method was 8%. The results obtained with both analytical methods are in reasonable agreement. It is worth

dx.doi.org/10.1021/ja3004914 | J. Am. Chem. Soc. 2012, 134, 5974−5984

Table 1. Percentages of DMFc Consumed during 1 min Two-Phase Reactions, Percentage of DMFc Used for Hydrogen Peroxide Production, and Total Number of transferred Electrons per Molecular oxygen Reduced in Two-Phase Experiments (2 mM DMFc and 100 μM Catalyst in DCB)

		NaI method		TiOx method	
system	electron donor consumed, %	n	$r_{H_2O_2}$, %	n	$r_{H_2O_2}$, %
Co_2(DPO) + DMFc	100	3.7	15	3.6	22
Co_2(DPOx) + DMFc	100	3.8	12	3.7	13
Co_2(DPX) + DMFc	100	3.9	7	3.7	16
CoTPP + DMFc	100	3.6	19	3.8	12
DMFc[a]	66	3.2	37	3.1	44
Co_2(DPOx) + DMFc[b]	100	3.8	11	3.8	8
Co_2(DPOx) + TTF	100	3.2	41	3.2	42
Co_2(DPOx) + TTF[a]	100	3.5	24	3.5	24

[a]Reaction time 10 min. [b]DCE as a solvent.

noting that a very low hydrogen peroxide concentration was observed for DMFc without any catalyst after 10 min, while the amount of hydrogen peroxide produced in the presence of CoTPP was lower than expected from the previous studies.[5,7] Solvent appears to have no significant effect on the selectivity of the catalyst, as similar results were obtained for the Co_2(DPOx) catalyzed oxygen reduction both in DCE and in DCB. When TTF was used as an electron donor, selectivity for hydrogen peroxide was 41% after 1 min (42% determined by TiOx method), but decreased to 24% after 10 min (both methods), indicating that Co_2(DPOx) catalyzes the decomposition of hydrogen peroxide as TTF is inactive toward hydrogen peroxide.[26] The differences in selectivity toward hydrogen peroxide (12% with DMFc, 41% with TTF) can be explained by the DMFc-catalyzed decomposition of hydrogen peroxide.

Oxygen reduction is quite fast with all of the catalysts, while it is very slow with TTF alone: 2 mL of 1 mM TTF in DCE in contact with 2 mL of 10 mM LiTB in 10 mM HCl had not reached completion after 80 h,[26] while the reaction with 2 mM TTF and 100 μM Co_2(DPOx) was finished in less than 60 s, as reported in this work. Also, all of the catalysts work significantly faster than the self-assembled "molecular rafts" of oppositely charged water-soluble porphyrins, cobalt tetramethylpyridinium porphyrin and cobalt tetrasulphonatophenyl porphyrin.[25] These rafts (50 μM in 10 mM HCl and 10 mM LiTB solution) were shown to catalyze oxygen reduction by 1 mM TTF in DCE with 78% selectivity toward water, reaching 96% conversion of TTF after one hour. The qualitative kinetic information obtained from these experiments is presented in Table 2, assuming a first-order reaction with respect to mediator (D) ($\nu = k_{app}[D]$). The rate constant could be calculated only for the reaction without any catalyst, but values for the other catalysts were estimated (see Supporting Information for calculation details). 100 μM of catalyst increases the reaction rate by more than a factor of 50−100. No difference in reaction kinetics was observed between DMFc and TTF, when Co_2(DPOx) was used as a catalyst, or between DCE and DCB.

Table 2. Conversion of Electron Donor (2 mM) at Different Times with Different Catalysts (100 μM), and the Estimated Rate Constants

catalyst	conversion (t = 30 s), %	conversion (t = 60 s), %	k_{app}, s^{-1}
Co_2(DPO)	100	100	>0.2
Co_2(DPOx)	100	100	>0.2
Co_2(DPX)	74	100	0.2−0.08
CoTPP	90	100	0.2−0.08
DMFc	25	66[a]	0.002

[a]Reaction time 10 min.

Although the contact time of hydrogen peroxide with the organic phase was less than 2 min, its decomposition was also investigated. A 1 mM H_2O_2 solution (in 10 mM HCl) was reacted with a 2 mM DMFc solution containing 1 mM CoTPP, and the hydrogen peroxide concentration was determined both before and after 2 min of reaction. During the reaction, hydrogen peroxide concentration decreased by ca. 5%, giving a first-order rate constant of $(3-4) \times 10^{-4}$ s^{-1}. After 1 h, most of the hydrogen peroxide had decomposed. When a solution containing Co_2(DPOx) instead of CoTPP was used, losses of hydrogen peroxide after 1 and 10 min were 11% and 34%, respectively, indicating that decomposition of H_2O_2 cannot be neglected over the total reaction time.

The hydrogen peroxide reduction was also investigated in an anaerobic glovebox. The concentration of hydrogen peroxide decreased by 46% during 1 min of reaction, as measured using the titanium oxalate method before and after the experiment. The color of the organic phase changed immediately, and no DMFc could be detected by voltammetry after completion of the reaction. Comparison of UV−vis spectra of the DCB phase after oxygen reduction under aerobic conditions and the biphasic reaction with hydrogen peroxide under anaerobic conditions are shown in the Supporting Information.

On the basis of these measurements, it seems that the species in the organic phase catalyzes the decomposition of hydrogen peroxide to molecular oxygen and water, and oxygen can be further reduced under biphasic conditions. Biphasic experiments with TTF show that Co_2(DPOx) catalyzes hydrogen peroxide decomposition and it seems to also be able to catalyze the reduction of H_2O_2 to water. Thus, selectivity toward water deduced from biphasic experiments is overestimated, especially at longer periods of time. The differentiation between hydrogen peroxide disproportionation to water and oxygen followed by four-electron oxygen reduction and the direct reduction of hydrogen peroxide by a two-electron process is very difficult. Therefore, a complete understanding of the catalyst selectivity cannot be achieved with these biphasic experiments. The best estimates of the catalyst selectivity toward hydrogen peroxide can be achieved with short reaction times, using TTF or another inactive redox species as a mediator. Ferrocene derivatives have been used as electron donors for oxygen reduction before,[7,27,42,43] but these results show that certain care has to be taken when determining the number of transferred electrons, and control experiments with hydrogen peroxide are necessary, especially in the case of stronger reductants like decamethylferrocene.

Previous studies have shown that in homogeneous conditions Co_2(DPX) produces water with 100% efficiency,[7] but when adsorbed on carbon, the selectivity decreases to 72%.[44] The selectivity reported in this work (93%, with DMFc)

dx.doi.org/10.1021/ja3004914 | J. Am. Chem. Soc. 2012, 134, 5974−5984

is better than previously reported for heterogeneous systems. At water−DCE interface, the selectivity of 50 μM Co_2(DPOx) toward four-electron reduction of oxygen by 1 mM TTF was reported to be 63% after 30 min of reaction,[25] which corresponds closely to the value of 76% reported in this work with 100 μM Co_2(DPX) and 2 mM TTF after 10 min of reaction. The enhanced selectivity observed in this work can be explained by a higher hydrogen peroxide decomposition rate with increasing catalyst concentrations.

Surprisingly low hydrogen peroxide yields were observed with CoTPP, as previous experiments with simple cobalt complexes have indicated that they only catalyze two-electron reduction of O_2.[5,7] Also, DFT calculations on cobalt porphine (CoP) support this finding,[45] and oxygen binding to CoTPP is not significantly different from CoP.[46] Formation of CoTPP dimers linked with molecular oxygen could explain the oxygen reduction to water instead of hydrogen peroxide, according to the mechanism described in Scheme S-2, but a simpler explanation would be the decomposition of produced hydrogen peroxide by DMFc and CoTPP. Four-electron reduction of molecular oxygen to water was also observed by Anson et al. in a thin benzonitrile layer, where both hydrogen peroxide and water were produced.[47]

Modeling. Structures presented in Scheme S-2 were optimized ("dock-in" path), together with those involving O_2, OOH, or H_2O_2 molecules "docked" on top of the Co_2(DPX) molecule ("dock-on" path) shown in Figure 7. All of the investigated species are described in Scheme 4. The oxidation states of the cobalt atoms are purely speculative. In some of the calculations, water molecules were added next to one of the cobalt atoms to mimic the Co_2(DPX) at the water−oil interface; solvent molecules on the oil side were not taken into account. In general, water appears to have only a small effect on the results.

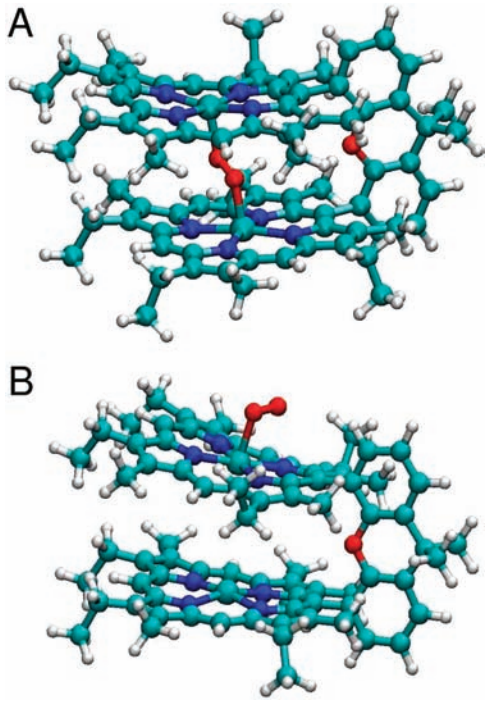

Figure 7. Optimized structures at the DFT-PBE level of inside ("dock-in" path) (A) and outside ("dock-on" path) (B) O_2 bonded Co_2(DPX) adducts.

Scheme 4. Complexes Investigated by DFT[a]

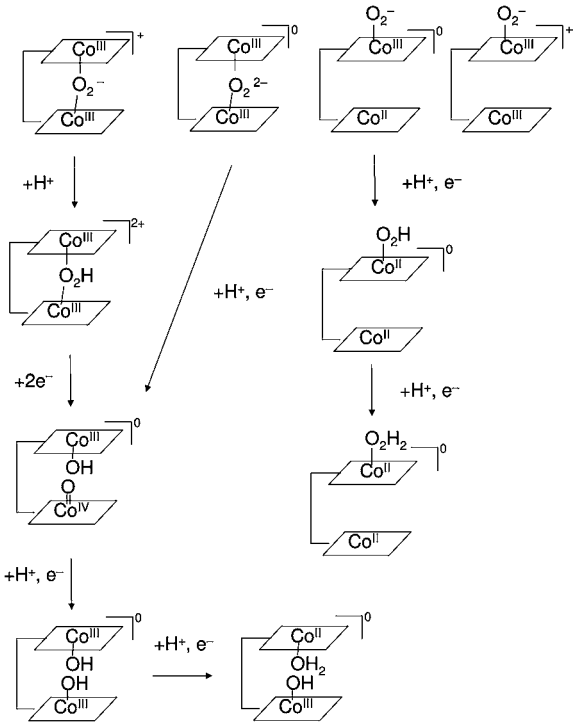

[a]The oxidation states of the cobalt atoms are purely speculative.

Molecular oxygen was placed inside the Co_2(DPX) molecule ("dock-in", Figure 7A), close to the cobalt atoms, and both neutral and +1 charged molecules were studied. In both cases, the O−O bond length was 1.33 Å, and the inclusion of water did not change the O−O distance (in z = +1 case, the distance was 1.34 Å). These results agree with the O−O distance of 1.35 Å reported in the literature for a +1 charged complex.[8] Additional water molecules had a very small role in oxygen binding, and the binding energy varied between 0.36 and 0.44 eV (Table 3). Calculations were also initiated from a broken O_2 molecule where the oxygen atoms were placed close to cobalt atoms with the O···O distance of ca. 3 Å. These structures converged to an O_2 molecule. Outside binding of O_2 on the Co_2(DPX) molecule (with z = 0 or +1) was also investigated ("dock-on", Figure 7B). For a +1 charged species, the binding energies were basically identical to those found when O_2 was located inside the Co_2(DPX) cavity ("dock-in"). For the neutral system, the binding energy difference was 0.3 eV favoring O_2 on Co_2(DPX). This is important for the H_2O_2 production as it is more likely that the O_2 will bind to Co_2(DPX) on the "exo" face. The O−O bond length inside the Co_2(DPX) molecule, d(O−O) = 1.33 Å, is much longer than observed in similar calculations with O_2 bound to normal Co porphyrins or at the

Table 3. Binding Energy of O_2 to Co_2(DPX) Computed at the DFT-PBE Level

	E_{bind}/eV			
	z = 0	z = +1	z = 0 + 3H_2O	z = +1 + 3H_2O
O_2 inside Co_2(DPX)	0.36	0.44	0.52	0.32
O_2 outside Co_2(DPX)	0.66	0.44		

dx.doi.org/10.1021/ja3004914 | J. Am. Chem. Soc. 2012, 134, 5974−5984

Scheme 5. "Dock-On/Dock-In" Mechanism for Oxygen Reduction Catalyzed by Cofacial Biscobalt Bisporphyrin Based on Computational and Experimental Results[a]

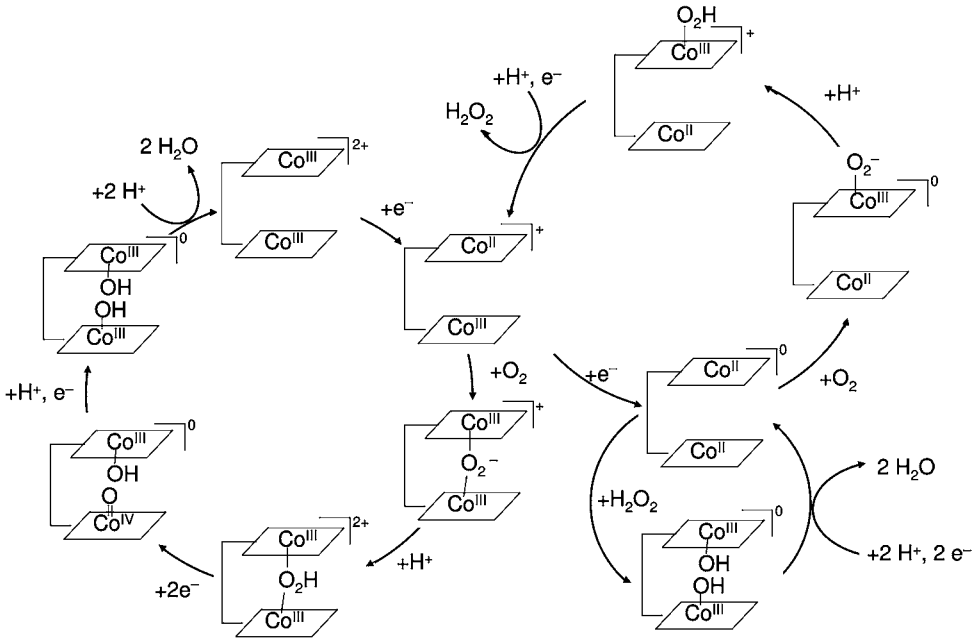

[a]The "dock-on" path on the top right shows the production of hydrogen peroxide on the catalyst, and the "dock-in" path on the left shows the production of water inside the catalyst. The first reduction step in the "dock-on" path can take place either before or after the complex formation with oxygen, because oxygen is also likely to bind on top of the $Co_2(DPX)^+$. The "dock-in" path down right shows the reduction of hydrogen peroxide inside the catalyst.

outer surface of $Co_2(DPX)$, $d(O-O)$ = 1.28 Å (z = 0) and 1.27 Å (z = +1). Sun et al. found an O−O distance of 1.289 Å when O_2 was bound to cobalt porphine.[45] Still, in all cases, O_2 was stable inside $Co_2(DPX)$.

In a second step, a proton (total charge +2) or hydrogen and an electron (total charge 0) were added to the O_2 system (see Schemes 4 and S-2). There are several possibilities in the presence of water close to one of the cobalt atoms: OOH can interact with either the O or the OH end orientated toward the Co atom, which binds water, or OOH can break and form an OHO type molecule. The latter turns out to be the most favorable case both in neutral and in +2 charged clusters. In all cases, an OHO type molecule was significantly lower in energy than OOH. In the neutral molecule, the OHO configuration was 0.6 eV lower in energy and in the +2 charged cluster the energy was 1.0 eV lower than that found for the OOH configuration. When OOH was broken, a hydrogen atom was added to it to form an OH−HO complex inside of $Co_2(DPX)$. Only a neutral complex was considered, as described in Scheme S-2. It is interesting to compare the energy to that of O_2 in $Co_2(DPX)$ + H_2. The reaction energy was 3.0 eV, strongly favoring the H_2 dissociation. Comparing this to $Co_2(DPX)$ + H_2O_2, OH−HO + $Co_2(DPX)$ is 1.8 eV lower in energy, confirming that $Co_2(DPX)$ can also dissociate H_2O_2. The addition of a proton and an electron to the system resulted in OH−H_2O in $Co_2(DPX)$. This structure was very stable, and the binding energy of water to $Co_2(DPX)$ was 0.90 eV. This is a very high binding energy, and thus the water stays inside $Co_2(DPX)$ for a long time.

Calculations of OOH on the surface of $Co_2(DPX)$ were interesting as it was clearly stable. We investigated if an OHO type molecule could reside on the $Co_2(DPX)$, but no such geometries were stable. The HOOH configuration on $Co_2(DPX)$ turned out to be quite stable. The binding energy of HOOH to $Co_2(DPX)$ was 0.29 eV, but HOOH on $Co_2(DPX)$ was 1.27 eV less stable than OH−HO inside $Co_2(DPX)$. It is also interesting to compare the formation energy of H_2O_2 from O_2 and H_2. This energy was 1.16 eV; thus H_2O_2 formation is highly probable on $Co_2(DPX)$.

The computational results suggest that addition of a proton or hydrogen to a O_2 molecule bound inside the $Co_2(DPX)$ cleft will split the O−O bond, leading to Co-bound O and OH groups, which at the next step evolve to two Co-bound OH groups and eventually to water ("dock-in"). The fate of the O_2 molecule interacting at the outer surface of the $Co_2(DPX)$ molecule is computationally less clear: OOH and HOOH adducts are stable, unlike OHO type configurations, but this is partly due to the lack of solvation of the OH group. However, we do not believe that a more accurate description of solvation would drastically change this picture. Experimental results show that the system will produce H_2O_2, but according to the computational results O_2 bound inside $Co_2(DPX)$ will be reduced to water. Thus, H_2O_2 comes from O_2 bound outside of $Co_2(DPX)$, following the "dock-on" path.

Another interesting observation was the O_2 binding energy to $Co_2(DPX)$. For +1 charged $Co_2(DPX)$, the binding energy was the same whether the O_2 was located inside or outside of the molecule. In the case of a neutral system, outside O_2 binding was 0.3 eV more favorable. Both of these results suggest that O_2 prefers to bind on the surface of $Co_2(DPX)$ because there are two binding sites outside the molecule, so the "dock-on" path will be favored over the "dock-in" path.

Because the catalyst is initially in a neutral form, oxygen will bind on the $Co_2(DPX)$, leading to hydrogen peroxide production. After desorption of H_2O_2 from the molecule, $Co_2(DPX)$ will have a +1 charge, as described in Scheme S-1.

dx.doi.org/10.1021/ja3004914 | J. Am. Chem. Soc. 2012, 134, 5974−5984

In this charge state, both binding processes, that is, either inside or outside the molecule, are equally favorable in terms of binding energy. Of course, $Co_2(DPX)^+$ can also be reduced by the mediator. Because the catalyst has been shown to produce water,[7,8] the reaction is also proceeding through the "dock-in" path. On the other hand, further reduction of hydrogen peroxide is also catalyzed by $Co_2(DPX)$, even though the reaction catalyzed by doubly linked cofacial porphyrin, Co_2FTF4, is reported to be slower than oxygen reduction.[48] The "dock-on/dock-in" mechanism for ORR and "dock-in" mechanism for H_2O_2 reduction are presented in Scheme 5. The first reduction step in the "dock-on" cycle can take place either before or after complex formation with oxygen, because oxygen is also likely to bind on the top of $Co_2(DPX)^+$. DMFc is also able to reduce $Co_2(DPX)^+$ to the neutral form.[7] Hydrogen peroxide reduction occurs by dissociation of HOOH and formation of a $Co^{III}-OH$ $HO-Co^{III}$ complex (also the intermediate of oxygen reduction inside the catalyst), followed by addition of two protons and two electrons ("dock-in" mechanism for H_2O_2 reduction).

Previously, the production of hydrogen peroxide has been assigned to reduction of the complex before protonation (dashed cycle in Scheme S-2),[8] as the active center of $[Co_2(DPX)-O_2]^+$ was calculated by DFT to be more basic than the trans-aryl substituted version $[Co_2(DPXM)-O_2]^+$, with $Co_2(DPXM)$ being less selective to four-electron reduction of molecular oxygen. However, these differences in observed selectivity could also be explained by the bulky aryl groups sterically hindering the "dock-in" path, thus favoring the "dock-on" path and leading to increased hydrogen peroxide production, as described by Scheme 5.

The 59% selectivity toward water obtained from a shake flask experiment with 100 μM $Co_2(DPOx)$ and 2 mM TTF after 60 s of reaction actually indicates that oxygen reduction takes place significantly through the "dock-on" path. Hydrogen peroxide generated by the "dock-on" path is subsequently reduced following the "dock-in" path, as described in Scheme 5. These results seem to be in disagreement with the experimental results obtained with "Pacman" porphyrins adsorbed on graphite electrodes,[8,48−50] but this disagreement can be explained by the large thermodynamic driving force. The standard potentials of oxygen reduction to H_2O_2 or H_2O were calculated to be 1.24 or 1.86 V vs SHE in DCB, respectively, while the standard potential of DMFc is 0.57 V vs SHE in DCB.[31] H_2O_2 generation is observed at higher overpotentials on ring-disk experiments with a cofacial porphyrin adsorbed on graphite, even when the four-electron reduction is taking place at lower overpotentials.[48] Thus, the driving force of oxygen reduction by DMFc or TTF is high enough to favor the "dock-on" path instead of the "dock-in" path.

These findings also disagree with the result obtained for homogeneous oxygen reduction catalyzed by $Co_2(DPX)$ in benzonitrile (BCN).[7] One explanation could be the difference in the thermodynamic driving force. The proton transfer from aqueous to oil phase is much easier for BCN ($\Delta_o^w G_{H^+}^0$ = 33 kJ/mol)[51] than for DCB or DCE ($\Delta_o^w G_H^0$ = 65 or 53 kJ/mol, respectively).[31] The calculated standard potentials for oxygen reduction to hydrogen peroxide or water are 0.98 or 1.53 V vs SHE in BCN, 0.36 V less than in DCB (see Supporting Information). This 0.36 V difference in the driving force probably plays a crucial role on the selectivity, so that the reaction proceeds through the "dock-in" path in BCN and "dock-on" path in DCB or DCE. Another reason for this disagreement may be as simple as the competitive coordination of the counterions and oxygen to the cobalt atoms. All of the earlier results have been obtained with more strongly coordinating anions (for example, ClO_4^-) as compared to TB^- used in this work.[52] It is well-known that anions that are noncoordinating in aqueous solution, such as ClO_4^-, NO_3^-, and BF_4^-, are found to be coordinating in nonaqueous solutions.[53,54] Thus, it is likely that coordination of perchlorate will compete with the coordination of oxygen on the catalyst, thus inhibiting the "dock-on" path, but weakly coordinating anions like TB^- are not able to bind to metal centers strongly enough to affect the oxygen binding. ClO_4^- also has a higher charge density than TB^-, so it associates more strongly with positively charged species by outer-sphere complexation. Also, benzonitrile can coordinate to the cobalt atoms, blocking the adsorption sites of oxygen, as it is more coordinative solvent than DCB.

To investigate the competition of ClO_4^- and BCN with O_2, calculations of their binding to the "dock-on" site of the $Co_2(DPX)$ molecule were perfomed. Both molecules are quite voluminous as compared to molecular oxygen, so binding to the "dock-in" site would be sterically hindered. The binding energy of BCN was found to be less than the value for oxygen (0.25 eV vs 0.44 eV for +1 charged porphyrin), confirming that the O_2 has higher binding probability, even though the concentration ratio between oxygen and BCN is roughly 10^{-4} (air saturated solution).[7] The binding of ClO_4^- is somewhat more problematic, as in all other calculations the coordinating molecule is neutral. The binding energy of ClO_4^- for neutral $Co_2(DPX)$ is very low (0.18 eV), but the ion−ion interaction of positive $Co_2(DPX)$ and ClO_4^- led to very high binding energy (2.6 eV). At long distance, this interaction is screened by the dielectric constant of the solvent, but obviously ClO_4^- even at very low concentration can compete effectively with the O_2 and thus promote "dock-in" path. Only one ClO_4^- anion can be bound to the $Co_2(DPX)^+$ (ClO_4^- has low binding energy to the neutral "dock-on" site), so the H_2O_2 cycle is only inhibited. On the other hand, the counteranion will bind on the Co^{III}-atom, thus complicating the electron transfer from the donor. As seen from Scheme 5, this is the critical point: accepting the electron from donor promotes "dock-on" path, but if this site is blocked by tightly bound perchlorate, "dock-in" path is promoted instead. The displacement of less strongly coordinating TB^- is easier than the displacement of perchlorate, and thus the "dock-on" path is also more active.

To translate these results in understanding biology, we can compare the structure of cytochrome *c* oxidase with the structure of cofacial porphyrins. In C*c*O, the central metal of the porphyrin ring is coordinated from below by histidine, so the protein structure prevents the coordination of oxygen outside the catalyst, thus blocking the "dock-on" path. This protection is important, as shown by our results. If the environment around the metal centers remains unprotected, hydrogen peroxide production will take place instead of the desired four-electron reduction, and hydrogen peroxide can be very harmful for proteins. Yet inside the catalyst, the hydrogen peroxide is safely dissociated by the metal centers and reduced to water. Thus, the next step in designing a bioinspired ORR catalyst would be to block the outer face of the porphyrin system.

dx.doi.org/10.1021/ja3004914 | J. Am. Chem. Soc. 2012, 134, 5974−5984

CONCLUSIONS

Electrochemistry at the interface between two immiscible electrolyte solutions is an excellent means to study bioinspired molecular catalysis of oxygen reduction. The results show that all of the catalysts studied produce both hydrogen peroxide and water. Therefore, the reaction environment has to be considered carefully to understand oxygen reduction in biological systems and to develop more selective catalysts for oxygen reduction. All of the catalysts increased the reaction rate significantly, by 2 orders of magnitude, but O_2 reduction catalyzed by Co_2(DPX) and CoTPP was slower than with the other tested systems. Co_2(DPX) has the highest selectivity for water (ca. 93%) with DMFc as a mediator, but the selectivity decreases to 59% if TTF is used instead. DFT calculations indicate that oxygen reduction proceeds significantly on the outside of the cofacial porphyrins, not only inside. The reaction product on the porphyrin is hydrogen peroxide, while the reduction inside the porphyrin results in formation of water. The selection of the catalyst is further complicated by both experimental and computational observations that cofacial porphyrins also catalyze the decomposition and/or reduction of hydrogen peroxide. The "dock-on/dock-in" mechanism is able to explain these results.

The advantage of four-electrode cell experiments is that they provide information about catalyst activity in PCET reactions. The results show that the oxygen complex formed with the cofacial "Pacman" porphyrin possessing a diphenylether linker, Co_2(DPOx)$-O_2$, has the highest affinity for protons in the PCET step, with the PCET wave already at the Galvani potential difference of 0.4 V. Other cofacial "Pacman" porphyrins exhibit similar behavior. The oxygen reduction was concluded to proceed through a PCET step, because it only took place in the simultaneous presence of a redox mediator, a catalyst, and oxygen.

These results help understanding why in biological systems the "outsides" of the active center are protected to avoid undesired side reactions. Simple model systems for their biological counterparts lacking this protection can thus produce quite unexpected results. The next step for improving these bioinspired oxygen reduction catalysts would be the synthesis of sheltered cofacial porphyrins.

ASSOCIATED CONTENT

Supporting Information

Oxygen reduction schemes proposed previously, voltammograms of cofacial porphyrins in the absence of a mediator, UV–vis spectra of DMFc and $DMFc^+$, comparison of UV–vis spectra of Co_2(DPOx) + DMFc after oxygen reduction and anaerobic hydrogen peroxide reduction, calculation of the Galvani potential difference and equilibrium concentrations in biphasic experiments, calculations of standard redox potentials of hydrogen evolution and oxygen reduction in benzonitrile, and estimations of the minimum value of the rate constants. This material is available free of charge via the Internet at http://pubs.acs.org.

AUTHOR INFORMATION

Corresponding Author

lasse.murtomaki@aalto.fi

Notes

The authors declare no competing financial interest.

ACKNOWLEDGMENTS

Financial support from Academy of Finland (Grant no. 133261) and European Cost Action D36/007/06 is acknowledged. The Centre National de la Recherche Scientifique (CNRS, UMR 6302), Swiss National Science Foundation, and NCCR MUST project are also gratefully acknowledged.

REFERENCES

(1) Jasinski, R. *Nature* **1964**, *201*, 1212–1213.
(2) Boulatov, R. In *N_4-Macrocyclic Metal Complexes*; Zagal, J. H., Bedioui, F., Dodelet, J.-P., Eds.; Springer: New York, 2006; pp 1–40.
(3) Dodelet, J.-P. In *N_4-Macrocyclic Metal Complexes*; Zagal, J. H., Bedioui, F., Dodelet, J.-P., Eds.; Springer: New York, 2006; pp 83–148.
(4) Zagal, J. H.; Paez, M. A.; Silva, J. F. In *N_4-Macrocyclic Metal Complexes*; Zagal, J. H., Bedioui, F., Dodelet, J.-P., Eds.; Springer: New York, 2006; pp 41–82.
(5) Fukuzumi, S.; Mochizuki, S.; Tanaka, T. *Inorg. Chem.* **1989**, *28*, 2459–2465.
(6) Fukuzumi, S.; Mochizuki, S.; Tanaka, T. *Chem. Lett.* **1989**, *18*, 27–30.
(7) Fukuzumi, S.; Okamoto, K.; Gros, C. P.; Guilard, R. *J. Am. Chem. Soc.* **2004**, *126*, 10441–10449.
(8) Chang, C. J.; Loh, Z. H.; Shi, C.; Anson, F. C.; Nocera, D. G. *J. Am. Chem. Soc.* **2004**, *126*, 10013–10020.
(9) Siegbahn, P. E. M.; Blomberg, M. R. A. *Chem. Rev.* **2010**, *110*, 7040–7061.
(10) Girault, H. H.; Schiffrin, D. J. In *Electroanalytical Chemistry*; Bard, A. J., Ed.; Marcel Dekker: New York, 1989; Vol. *15*, pp 1–142.
(11) Kihara, S. In *Interfacial Nanochemistry. Molecular Science and Engineering at Liquid–Liquid Interfaces*; Watarai, H., Teramae, N., Sawada, T., Eds.; Springer: New York, 2005; pp 127–154.
(12) Cunnane, V. J.; Geblewicz, G.; Schiffrin, D. J. *Electrochim. Acta* **1995**, *40*, 3005–3014.
(13) Liljeroth, P.; Quinn, B. M.; Kontturi, K. *Langmuir* **2003**, *19*, 5121–5127.
(14) Ohde, H.; Maeda, K.; Yoshida, Y.; Kihara, S. *J. Electroanal. Chem.* **2000**, *483*, 108–116.
(15) Suzuki, M.; Matsui, M.; Kihara, S. *J. Electroanal. Chem.* **1997**, *438*, 147–151.
(16) Su, B.; Partovi-Nia, R.; Li, F.; Hojeij, M.; Prudent, M.; Corminboeuf, C.; Samec, Z.; Girault, H. H. *Angew. Chem., Int. Ed.* **2008**, *47*, 4675–4678.
(17) Su, B.; Hatay, I.; Li, F.; Partovi-Nia, R.; Méndez, M. A.; Samec, Z.; Ersoz, M.; Girault, H. H. *J. Electroanal. Chem.* **2010**, *639*, 102–108.
(18) Hatay, I.; Su, B.; Li, F.; Méndez, M. A.; Khoury, T.; Gros, C. P.; Barbe, J. M.; Ersoz, M.; Samec, Z.; Girault, H. H. *J. Am. Chem. Soc.* **2009**, *131*, 13453–13459.
(19) Partovi-Nia, R.; Su, B.; Li, F.; Gros, C. P.; Barbe, J. M.; Samec, Z.; Girault, H. H. *Chem.-Eur. J.* **2009**, *15*, 2335–2340.
(20) Trojánek, A.; Langmaier, J.; Su, B.; Girault, H. H.; Samec, Z. *Electrochem. Commun.* **2009**, *11*, 1940–1943.
(21) Hatay, I.; Su, B.; Méndez, M. A.; Corminboeuf, C.; Khoury, T.; Gros, C. P.; Bourdillon, M.; Meyer, M.; Barbe, J. M.; Ersoz, M.; Záliš, S.; Samec, Z.; Girault, H. H. *J. Am. Chem. Soc.* **2010**, *132*, 13733–13741.
(22) Su, B.; Hatay, I.; Trojánek, A.; Samec, Z.; Khoury, T.; Gros, C. P.; Barbe, J. M.; Daina, A.; Carrupt, P. A.; Girault, H. H. *J. Am. Chem. Soc.* **2010**, *132*, 2655–2662.
(23) Trojánek, A.; Mareček, V.; Jänchenová, H.; Samec, Z. *Electrochem. Commun.* **2007**, *9*, 2185–2190.
(24) Partovi-Nia, R. Ph.D. Thesis, Ecole Polytechnique Fédérale de Lausanne, Switzerland, 2010.
(25) Olaya, A. J.; Schaming, D.; Brevet, P.-F.; Nagatani, H.; Zimmermann, T.; Vanicek, J.; Xu, H.-J.; Gros, C. P.; Barbe, J.-M.; Girault, H. H. *J. Am. Chem. Soc.* **2012**, *134*, 498–506.
(26) Olaya, A. J.; Ge, P.; Gonthier, J. F.; Pechy, P.; Corminboeuf, C.; Girault, H. H. *J. Am. Chem. Soc.* **2011**, *133*, 12115–12123.

(27) Lubach, J.; Drenth, W. *Recl. Trav. Chim. Pays-Bas* **1973**, *92*, 586−592.
(28) Buchler, J. W. In *The Porphyrins*; Dolphin, D., Ed.; Academic Press: New York, 1978; Vol. *1*, pp 389−483.
(29) Fermín, D. J.; Duong, H. D.; Ding, Z.; Brevet, P. F.; Girault, H. H. *Phys. Chem. Chem. Phys.* **1999**, *1*, 1461−1467.
(30) Hundhammer, B.; Müller, C.; Solomon, T.; Alemu, H.; Hassen, H. *J. Electroanal. Chem.* **1991**, *319*, 125−135.
(31) Peljo, P.; Rauhala, T.; Murtomäki, L.; Kallio, T.; Kontturi, K. *Int. J. Hydrogen Energy* **2011**, *36*, 10033−10043.
(32) Partovi Nia, R.; Su, B.; Méndez, M. A.; Barbe, J. M.; Samec, Z.; Girault, H. H. *J. Electroanal. Chem.* **2011**, *656*, 147−151.
(33) Sellers, R. M. *The Analyst* **1980**, *105*, 950−954.
(34) Battino, R.; Rettich, T. R.; Tominaga, T. *J. Phys. Chem. Ref. Data* **1983**, *12*, 163−178.
(35) Luehring, P.; Schumpe, A. *J. Chem. Eng. Data* **1989**, *34*, 250−252.
(36) Gao, F.; Yang, Y.; Liu, J.; Shao, H. *Ionics* **2010**, *16*, 45−50.
(37) Mortensen, J. J.; Hansen, L. B.; Jacobsen, K. W. *Phys. Rev. B* **2005**, *71*, 1−11 ; https://wiki.fysik.dtu.dk/gpaw/.
(38) Perdew, J. P.; Burke, K.; Ernzerhof, M. *Phys. Rev. Lett.* **1996**, *77*, 3865−3868.
(39) Cramer, C. J. *Essentials of Computational Chemistry*, 2nd ed.; John Wiley & Sons Ltd.: Chichester, 2004.
(40) Blöchl, P. E. *Phys. Rev. B* **1994**, *50*, 17953−17979.
(41) Méndez, M. A.; Partovi-Nia, R.; Hatay, I.; Su, B.; Ge, P.; Olaya, A.; Younan, N.; Hojeij, M.; Girault, H. H. *Phys. Chem. Chem. Phys.* **2010**, *12*, 15163−15171.
(42) Halime, Z.; Kotani, H.; Li, Y.; Fukuzumi, S.; Karlin, K. D. *Proc. Natl. Acad. Sci. U.S.A.* **2011**, *108*, 13990−13994.
(43) Fukuzumi, S.; Kotani, H.; Lucas, H. R.; Doi, K.; Suenobu, T.; Peterson, R. L.; Karlin, K. D. *J. Am. Chem. Soc.* **2010**, *132*, 6874−6875.
(44) Chang, C. J.; Deng, Y.; Shi, C.; Chang, C. K.; Anson, F. C.; Nocera, D. G. *Chem. Commun.* **2000**, 1355−1356.
(45) Sun, S.; Jiang, N.; Xia, D. *J. Phys. Chem. C* **2011**, *115*, 9511−9517.
(46) Zheng, S.; Jiujun, Z. *J. Phys. Chem. C* **2007**, *111*, 7084−7090.
(47) Chung, T. D.; Anson, F. C. *J. Electroanal. Chem.* **2001**, *508*, 115−122.
(48) Collman, J. P.; Hendricks, N. H.; Leidner, C. R.; Ngameni, E.; L'Her, M. *Inorg. Chem.* **1988**, *27*, 387−393.
(49) Durand, R. R. Jr.; Bencosme, C. S.; Collman, J. P.; Anson, F. C. *J. Am. Chem. Soc.* **1983**, *105*, 2710−2718.
(50) Collman, J. P.; Denisevich, P.; Konai, Y.; Marrocco, M.; Koval, C.; Anson, F. C. *J. Am. Chem. Soc.* **1980**, *102*, 6027−6036.
(51) Chung, T. D.; Anson, F. C. *Anal. Chem.* **2000**, *73*, 337−342.
(52) Geiger, W. E.; Barrière, F. *Acc. Chem. Res.* **2010**, *43*, 1030−1039.
(53) Rosenthal, M. R. *J. Chem. Educ.* **1973**, *50*, 331.
(54) Strauss, S. H. *Chem. Rev.* **1993**, *93*, 927−942.